Synthesis of multifunctional nano-drug with targeted delivery for the synergistic pathway of various inducers on inhibition of breast cancer cell line

Shaghyegh Shafighi
Islamic Azad University
Mohammad Zaefizadeh (mzaefi@iauardebil.ac.ir)
Islamic Azad University
Behbood Jaafari
Islamic Azad University
Mohammad Reza Alivand
Medical College of Wisconsin
Saeed Ghorbian
Islamic Azad University

Article

Keywords: oleuropein, quercetin, coumarin, valproic acid, apoptosis, MCF7, magnetic nanoparticles

Posted Date: September 12th, 2023

DOI: https://doi.org/10.21203/rs.3.rs-3309260/v1

Abstract

Background and objective: In recent years, interest has grown in the anti-cancer properties of natural compounds, particularly polyphenols including, Oleuropein, Quercetin, Coumarin (an aromatase inhibitor) and Valproic acid, with fewer side effects. Oleuropein stops the cell cycle in the G2/M phase by inhibiting metalloproteinase and increasing the expression of some caspases. Quercetin induces apoptosis by reducing the activity of the PI3K/Akt/IKK-/NF-B pathway. Valproic acid is an inhibitor of histone deacetylases which has a vital role in preventing the spread and progression of cancer. However, the therapeutic effects of polyphenols have constrained by their poor bioavailability. The goal of this study was creation of a natural magnetic nano-complex that is more bioavailable to examine how oleuropein, quercetin, coumarin, and valproic acid work in concert to limit cell growth.

Methods: In this work, a silicon bridge (sio-N-) was built using nano-magnetic iron and methoxy silane to create a magnetic nano-complex with four plant-derived substances: oleuropein, coumarin, quercetin, and valproic acid. These complexes were then analyzed using a variety of spectroscopic and size measures. Then, using the MTT technique and real-time PCR, the inhibitory impact and expression of apoptotic genes on the MCF7 cell line was assessed.

Results: FT-IR, SEM, TEM, EDX, XRD, DLS, and VSM techniques used to validate the synthesis of the nano-complex. The magnetic nano-complex exhibits a greater level of toxicity than the quadruple compound without nanoparticles, according to the MTT test findings. Moreover, compared to any of the materials or their combinations, the magnetic quadruple nanocomposite dramatically reduced the inhibition of cancer cells. Hoechst staining and flow cytometry cell techniques used to confirm this assumption. The quadruple combination and quadruple nanocomposite of magnetism induced overexpression of p53, bim, and bak and reduced BCL2 expression, according to real-time PCR data. Thus, our results showed that the nano-complex treatment increased the expression level of genes involved in apoptosis by up to two times.

Conclusion: Using plant-derived materials with various properties attached to magnetic nanoparticles can increase their toxicity against breast cancer cells and increase their concentration in the cell. Additionally, by creating a synergistic effect through various molecular pathways, it inhibits the proliferation of cancer cells and causes them to undergo apoptosis.

Introduction

The most prevalent disease in women is breast cancer, which had 2,261,419 cases and 684,996 fatalities in 2020 (1). Current treatment approaches, including as surgery, chemotherapy, radiation therapy, and immunotherapy, have limitations and downsides. The toxicity of chemotherapy on normal cells, severe side effects, and innate or acquired drug resistance have all reduced the effectiveness of medications. (2, 3).

The tumors from breast cancer are a remarkably diverse/heterogeneous mass. To maintain cell homeostasis, normal breast cells must maintain a balance between cell proliferation and apoptosis. When this balance is perturbed, the anti-apoptotic signaling pathway is activated, and the expression of pro-apoptotic enzymes decreases, which can result in uncontrolled proliferation of cells, treatment resistance, and cell relapse (4–6). The Bcl2 gene family, which produces proteins that may either promote or prevent apoptosis, is linked to the primary mechanism for apoptosis in breast cells. Bax, Bak, Bad, and Bclxs are pro-apoptotic proteins, whereas Bcl2 and BclxL are anti-apoptotic.

About 80% of breast cancer cells in human beings express Bcl2, which has been associated with the expression of estrogen and progesterone receptors and provides a favorable prognosis for the disease (7). The p53 protein controls cellular processes related to DNA repair, the cell cycle, and apoptosis. According to previous studies, this gene's mutations or high protein expression linked to a poor prognosis for breast cancer. It is widely known that chemotherapy induces apoptosis through p53-dependent pathways. As passive zymogens (inactive enzymes) that are activated by cleavage via an intracellular proteolytic cascade, caspases can serve as both initiators and effectors of the apoptotic pathway (5).

Numerous studies have shown that a special class of natural compounds targets signalling pathways that are crucial for the development, treatment, and apoptosis of cancer because of their unique biological characteristics and absence of harmful side effects (8, 9). Phenolic compounds are among the naturally occurring substances found in the Mediterranean diet that are effective in regulating the interactions between growth factor receptors, and cell signaling cascades like PI3K, Akt, mTOR, RAS, and MAPK, as well as the expression of genes involved in cycle arrest. Apoptosis, cell death, and cell survival all have anticancer effects (10, 11). Consuming polyphenols as part of a healthy diet or as a dietary supplement is helpful in preventing breast cancer. High concentrations of polyphenols can inhibit the growth of ER- and ER + BC cells, whereas lesser doses can even stimulate cell growth. Encouraging ER + cells (12). In breast cancer cell lines, a polyphenol complex's anticancer characteristics were revealed to exhibit anti-metastatic effects via inhibiting the JAK2/STAT3 and Wnt pathways and encouraging apoptosis (13).

The therapeutic advantages of phenolic compounds as therapy have been restricted despite their strong anticancer capabilities (14, 15). These drawbacks include limited bioavailability, low solubility, poor permeability, instability, and fast release of chemicals.

According to evidence, using nanotechnology is the most effective way to improve the bioavailability of phenolic chemicals (10). Nanotechnology increases the bioavailability and bioactivity of herbal medicines by lowering the size of the particle, altering the surface, and entrapping the drug. Utilizing nanoparticles to deliver polyphenols to specific tissues and reduce their immunogenicity may boost their efficacy (16).

Due to better-targeted therapy, increased stability, better anti-neoplastic activity, improved pro-apoptotic activity against tumor cells, higher intracellular concentration, and slow release, nano-formulation of natural polyphenols leads to more effective cancer prevention and treatment (17). One of the most

outstanding possibilities for drug delivery carriers in nanotechnology is magnetic nano-particles, since they prolong drug presence, increase efficacy, reduce drug toxicity in healthy cells, and lessen cancer cells' resistance to cytotoxic drugs that are crucial to their precise distribution (18). Given their high bioavailability and low toxicity, magnetic nano-particles are being used more frequently in targeted therapeutics. These particles are made of magnetite and maghemitite-derived iron oxide nanoparticles. In general, magnetic nanoparticles have characteristics that make them perfect for magnetic field-based distribution to target regions (19).

Oleuropein (OLE), a naturally occurring polyphenol and the most significant phenolic ingredient in olives, functions by blocking cells in the G2/M phase of the cell cycle, which slows tumor growth and is the primary reason for olives' anticancer qualities. Additionally, OLE controls cancer through epigenetic mechanisms, including inhibiting HDAC. Oleuropein suppresses the growth of MCF7 cells, significantly increases death induction, and promotes apoptosis in the AGS cell line in its nano-magnetic form (20).

Another polyphenolic substance with known anticancer effects is coumarin. Cancer pathways including cell cycle arrest, angiogenesis inhibition, kinase inhibition, aromatase inhibition, telomerase inhibition, and sulfatase inhibition are all involved in the impact of coumarin and its metabolites on cancer cell lines including MCF-7, ACHN, HL-60, and H727. Heat shock protein and cell death induction possess cytostatic functions (21, 22). Coumarins' caspase-dependent induction of apoptosis exerts an anti-proliferative impact by suppressing the expression of Bcl2 in multiple organs and tissues (23). According to research studies, nanocoumarin is more effective and powerful than synthetic coumarin at reducing the production of p53, Cyclin D1, Survivin, and Stat-3. This is most likely because the encapsulated form is more readily absorbed by cells (24).

The anticancer effects of polyphenolic flavonoids have also been proven in vitro and in animal models with antioxidant activity, effective on the expression of detoxifying enzymes, and modulation of the protein signalling cascade (25). Quercetin (3, 3, 4, 5, 7-pentahydroxy Flavon) is one of the flavonoid compounds that have been demonstrated to induce apoptosis through the mitochondrial route linked with the downregulation of the activity of the PI3K/Akt/NF-κB pathway. In fact, quercetin suppresses the phosphorylation of Akt and IKK-a, and hinders the nuclear translocation and activation of the NF-κB transcription factor (26). According to studies, quercetin's high encapsulation efficiency, lengthy circulation duration, tumour targeting, and inhibitory actions are all enhanced by its incorporation into nanoparticles. Quercetin would also be undetectable when used with other anticancer medications like doxorubicin and paclitaxel in a tumour carrier (27).

One of the most popular histone deacetylase inhibitors, valproic acid, has been demonstrated to have antitumor effects on a variety of solid tumors (15, 28) and to be useful in the treatment of a variety of human malignancies, including breast cancer. It has been shown to drastically slow down cell development and cause G0/G1 arrest, which results in apoptotic cell death in MDA-MB-231 TNBC cells (27). Targeted therapy may be possible thanks to the multifunctionality of natural compounds and their synergistic action against a variety of illnesses, including breast cancer, as well as the unique properties

of magnetic nanoparticles. Therefore, we may expect for the therapy of breast cancer the targeted transfer of the aforementioned natural compounds concurrently with the activation of apoptosis, stopping the cell cycle, antioxidant effects, and lowering cytotoxicity. Designing novel drug delivery systems (NDDS) using passive and active targeting mechanisms can increase the effectiveness of anticancer medications while reducing their systemic toxicity. The transfer of the synthetic quadruple magnetic anticancer nano-complex to MCF7 cancer cells was the main objective of this study in order to assess its impact on the expression of genes that are useful for preventing cell growth and causing apoptosis in breast cancer cells.

Results

Examining the synthesized complex's mechanism

Figure 1 shows the composition of the 3-aminopropyltrimethoxysilane-modified magnetite nanoparticles in the state where they are attached to the quadruple compound, which includes nanooleuropein, nanocoumarin, nanovalproic acid, and nanoquercetin. Methoxysilane is shown individually. The development of the quadruple complex and the production of the quadruple magnetic nano-complex of oleorepin, coumarin, quercetin, and valproic acid are demonstrated by the presence of unique peaks of each substance.

Figure 1:

The crystallinity of the nanoparticles and the synthesized complex confirms that the magnetic nanoparticles modified with 3-aminopropyltrimethoxysilane coupled with valproic acid, oleuropein, quercetin, and coumarin conform to the given data of standard XRD patterns (JCPDS card No. 86-2267) (Fig. 2). The saturation magnetization of magnetite iron oxide nanoparticles modified with 3-aminopropyltrimethoxysilane in the state connected to the quadruple complex is shown by the VSM magnetization curve in terms of the field, which exhibits the presence of a single-domain magnetic material without a residual loop—approximately 80 emu/g. The material encasing the magnetic core is causing the new lowering shift in the hysteresis loop seen in Fig. 3.

Figure 2 & 3

By applying the Debye-Scherr formula to the width of the longest peak at half height in an X-ray diffraction analysis, the average particle size was determined to be 23.45 nm for magnetite nanoparticles without modification and 35.45 nm for those modified with 3-aminopropyltrimethoxysilane attached to compound 4.

The SEM and EDAX pictures of magnetite nanoparticles modified with 3-aminopropyltrimethoxysilane connected to oleuropein, coumarin, valproic acid, and quercetin at a 100 nm magnification are shown in Figs. 4 and 5, respectively. Spherical nanoparticles are properly distributed and uniformly distributed in EDAX and SEM images.

Figure 4 & 5

The TEM image (Fig. 6) illustrates the magnetic core and surrounding material and confirms the particle size determined by the SEM. DLS was used to measure the synthesized nanoparticle's size (Fig. 7), and the resultant size was determined to be 44.5.

Figure 6&7

Cell viability assay (MTT)

On MCF-7 cells, the MTT test was used to analyze the effects of various doses of the compounds under investigation (Table 2). When comparing the treatments, the vitality of mcf7 cells varied significantly (P value = 0.01).

Table 1
Sequence of primers used to perform qRT-PCR

Gene	Primer Sequence (5'-3')	PCR Product length (bp)
Caspase 8 forward	AAGTGCCCTTCCCTTGCTG	153
Caspase 8 reverse	GCAGAAAGTCAGCCTCATCC	
Caspase 9 forward	AAAGTTGTCGAAGCCAACCC	158
Caspase 9 reverse	GACTCACGGCAGAAGTTCAC	
BCL2 forward	TGTGGCCTTCTTTGAGTTCG	162
BCL2 reverse	CCTACCCAGCCTCCGTTATC	
P53 forward	AGGTTGGCTCTGACTGTACC	162
P53 reverse	GATTCTCTTCCTCTGTGCGC	
BAK forward	CAATGTCCTCCCTGCTGTTG	167
BAK reverse	AGAACCACACCCAGAACCAC	
BIM forward	AGTTCTGAGTGTGACCGAGA	156
BIM reverse	AGGAGGACTTGGGGTTTGTG	

Table 2
Results of the MTT test on MCF-7 cells for various concentrations of the investigated materials

S.OV	Df	Nano Iron	Quadruple nano-complex in MCF7	Quadruple nano-complex in Fibroblast cells
treatment (concentration)	8	32ns	**734.51	57.6*
Test error	9	19.55	25.45	16.87
*P < 0.05				
** Significance at less than 1%				

Using AAT Bioquest's online programme, the LC50 for quadruple nano-complex and quadruple physical combinations was calculated (Fig. 8, 9). The quadruple compound's LC50 concentration was 644.654 g/ml, whereas the quadruple nano-complex's was 264.6226 g/ml.

Figure 8 & 9

The relative expression of genes in treated cells by Real-time PCR

The relative expression levels of the examined genes in comparison to the housekeeping gene GAPDH2 were ascertained by using the Real-time PCR technique.

Figure 11

P53, BCL2, BAK, Bim, and caspase 8 genes showed a significant difference between the treated cells and control samples in terms of gene expression at a probability level of less than 1% (P-value < 0. 01), while the caspase 9 gene showed the same expression in both cells (Fig. 10E). Oleuropein, coumarin, and quercetin treated cells showed the same expression. Only the BCL2 gene showed a decrease in expression level at mRNA level, and this was most pronounced when valproic acid and triple nano complex were used as nanomagnets. The rise in expression was detected in the P53, BAK, Bim, caspase 8, and caspase 9 genes (Fig. 10B). When the four substances under study were treated as formulated nanomagnets, the p53 gene experienced the highest increase in expression, which was 2.76 times higher and statistically significant compared to the control (Fig. 10A). For the BAK gene, the same result was observed (Figure-10C). The treatment with the quadruple magnetic nano-complex and healthy cells showed the greatest increases in expression, whereas the substantial treatment with coumarin at LC50 showed a lesser rise in expression than the control treatment. The simultaneous application of a nano-complex comprising four magnetic materials dramatically enhanced the expression of the bim gene by 1.76 times, with the healthy control showing the greatest expression (2.63 times) (Fig. 10D). Caspase 8 expression was most strongly induced by oleuropein treatment, and it was significantly increased by 1.94 times when four substances were administered simultaneously in treatment. The highest increase was observed when the four substances under study were added together to serve as nanomagnets, which

resulted in the highest induction of expression. In comparison to the control, its expression was 1.98 times more significant (Figure – 10F).

Oleuropein, quadruple magnetic nano-complex, and valproic acid treatment, among the four different treatments examined, all successfully inhibited MCF7 cancer cells by inducing internal apoptosis through caspase 9 and external apoptosis through procaspase 9. As a result, it can be claimed that the expression level of apoptotic genes was greater and their LC50 inhibitory concentration was lower in the form of nanoformulation. Cellular techniques and Hoechst staining in the treated cells were used to confirm apoptosis (Fig. 11).

Figure 11

Discussion

Due to the medicinal characteristics of cells, steady cellular and molecular changes, aberrant expression of cancer cell surface chemicals, limited cell permeability, low concentration in cells, and the destruction of healthy cells, chemotherapy medications were unable to effectively treat cancer. Due to their anti-cancer and antioxidant characteristics, as well as their minimal negative effects on healthy cells, natural chemicals, particularly polyphenolic compounds, constitute one of the most varied classes of plant secondary metabolites and have caught the interest of researchers working on cancer treatments. However, their limited bioavailability makes them difficult to treat tumours. By passively targeting cancer cells, increasing anti-neoplastic activity, and improving bioavailability, nanofabrication has been demonstrated to increase the anti-cancer properties of natural polyphenols (29). Researchers are interested in nanomagnets as a targeted carrier with a magnetic field, but they are also concerned about the health hazards posed by their toxicity, which may be reduced by altering the ambient conditions during the synthesis of nanomaterials (30). The fundamental mechanism of nanomaterials' anti-tumor activities is based on interactions between magneto-mechanical and magneto-chemical systems, which affect the structure of loaded agents and alter the redox state of tumors by producing ROS (31). In this work, four substances—oleuropein, coumarin, quercetin, and valproic acid—were attached to nano-magnetic iron concurrently by an NH silica bridge, and the synthesis was verified by a TEM picture and EDAX compliance with the standard of connected substances. The same technique, which was congruent with the findings of this study, has been utilised to synthesise magnetic nano oleuropein (18), curcumin (32), and other natural compounds. Observations revealed that doxorubicin may penetrate nanoFe3O4 coated with tetraheptylammonium more deeply into cancer cells through internal endocytosis mechanisms, increasing the amount of drug absorbed by the corresponding K562 leukaemia cells significantly (33). Furthermore, research has demonstrated that magnetic iron oxide nanoparticles suppress lung cancer cells by triggering death by raising caspase 3 activity (34). This study demonstrated that the quadruple magnetic nanocomposite significantly reduced the concentration required to inhibit cancer cells compared to any other material or material combination. The inhibition of 50% of the nanostructure in valproic acid, or roughly twice as much, resulted in the greatest concentration reduction. Caspase 9's expression was raised by valproic acid, however Caspase 8's was not. This

indicates that the internal mitochondrial route was adopted to induce apoptosis. This finding was anticipated since the acetylation of histones and subsequent production of caspase are two processes that contribute to the induction of apoptosis (35).

Oleuropein has been found to have an impact on the expression of most genes, including those for cytokines, transcription factors, adhesion molecules, chemokines, growth factor receptors, and inflammatory enzymes (36). Oleuropein was recently reported to control the NF-B activation cascade, which results in the onset of apoptosis in breast cancer cells (37). According to a study by Barzegar et al., magnetic nano oleuropein increased the expression of the Kras gene, which in turn caused apoptosis and necrosis in AGS gastric cancer cells. Overexpression of the K-ras gene led to in the overexpression of the p53 gene, which balanced the expression of the K genes and inhibited the proliferation of cancer cells (18).

According to the results of this study, quercetin did not significantly affect the induction of death by caspases 8 and 9, but the rise in the Bim and BAK genes and the severe drop in BCl2 support the use of quercetin in a different manner to suppress cancer cells. While nano-quercetin is non-cytotoxic to keratinocytes at concentrations lower than 250 ng/ml, it is known to be toxic to normal cells (38). In comparison to bulk quercetin at all dosages, nano quercetin exhibited the effects of apoptosis, mitochondrial malfunction, caspase activation, and G2 phase cell cycle arrest (39). This suggests that nano quercetin may have therapeutic potential for cervical and breast cancer.

A number of active mechanisms, including the induction of apoptosis through PI3K, concurrent caspase-mediated reduction of p-Akt, and enhanced activation of carcinogenic FoxO1, have been investigated in previous studies to demonstrate the inhibitory impact of quercetin in cervical and breast cancer (40). However, further examination needs to be conducted. Successful therapeutic development depends on understanding fundamental signaling pathways and how these nanoquercetins affect other cancer-related disorders through clinical research. In this work, the plant polyphenol coumarin caused apoptosis by increasing caspase 9, which was supported by increased levels of bim, p53, and bak and decreased levels of Bcl2. Coumarin's ability to inhibit the MCF7 cell line was accomplished via upregulating procaspase 9.

This route was reinforced by the decline in Bcl2 expression and the rise in Bak, Bim, and P53. After Coumarin therapy, there was a substantial drop in Bcl-2 gene expression and an increase in Bax gene expression, which is indicative of a decrease in the Bcl2-/Bax ratio, which can result in the activation of the apoptotic protein caspase (41). According to reports, aromatase inhibitors enhance signalling for cell death and suppress cell growth (42). In conclusion, our research shown that Coumarin specifically suppresses the growth of MCF-7 breast cancer cells and causes cell cycle arrest, which activates apoptosis.

At a dosage of 664 g/ml, the triple compound killed 50% of MCF7 cancer cells in vitro. If its nanostructure was able to block 50% of the MCF7 cell line at a dose of 264 g/ml. As evidenced by the fact that consumption was decreased by 2.5 times the inhibitory concentration of 50%, this study demonstrates

the critical function that reduction in consumption plays in the manufacture of the examined pharmaceuticals in nano form. The capacity of the nano structure to enter the cells from one side and transfer values may be the cause of this. Because nanoparticles have a larger surface area, it is high. This result was consistent with earlier studies (38, 39).

Two lines of research were carried out to examine the inhibitory mechanism of MCF7 cancer cells. Hoechst staining was employed to demonstrate that the first aspect of the analysis—cell apoptosis—was correct (Fig. 11). Oleuropein promotes apoptosis by caspase 8 according to the results of analyzing the expression of genes in various treatments, which were supported by the overexpression of p53, bim, bak, and the decrease in BCL2 expression. Additionally, oleuropein administration resulted in caspase-9-mediated apoptosis activation.

This pattern was also present in the quadruple compound and quadruple magnetic nanocomposite treatments, however the level of apoptosis inducer expression was stronger in the nano treatment. It was indicated in the procaspase 8 and 9 (internal and external routes) triple combination therapy, which demonstrates the additive and cumulative effects of drugs with various qualities. However, the induction of apoptosis at a lower dose, the overexpression of caspases, and the support of other genes active in apoptosis enhanced when this chemical was manufactured in a nanoform. As a result, after nanotreatment, the expression level of overexpressed genes in apoptosis can be found to rise by up to twice.

Materials and methods

Synthesis of nano-complex

The four natural compounds used in our research—oleuropein, quercetin, coumarin, and valpyrroic acid—were obtained from Sigma Aldrich in order to create the quadruple anticancer nano-complex. We bought ready to use US-Nano magnetite (Fe_3O_4) nanoparticles. Prior to binding the amino group on the iron oxide magnetite nanoparticles via shaking method, the 3-aminopropyltrimethoxysilane was utilized as an intermediate to suspend the magnetite particles in ethanol. Methoxy groups leave the substance during this process, Si-O-Si bonds form, and then the aminopropyl group is linked to the surface of the magnetite nanoparticles. The preparation of coumarin, quercetin, and valpyric acid powder (Sigma firm) required a 14 mM solution of 96% ethanol. Through the use of FT-IR, SEM, TEM, EDX, XRD, DLS, and VSM techniques, the synthesis of nano-complexes was verified.

Cell Culture

MCF7 cells were bought from the Pasteur Institute cell bank in Tehran, Iran, for the purpose of this experimental work. The cells were maintained in an incubator at 37°C, 5% CO_2, and 95% humidity while being grown in PRMI1640 culture media with 10% fetal bovine serum (FBS) and 1% penicillin/streptomycin.

Toxicity of magnetic quadruple nano-complex by MTT assay

In each of the 96 wells, MCF7 cells were first cultured. Cells in wells with a capacity of 100 microliters were added, and the wells were cultured for 24 hours with various doses of nano-complex (12.5-25-50-100 micrograms). Then, each well received 5 mg/ml of the MTT solution, and after 4 hours of incubation, DMSO solution was added. Afterward, the LC50 for various concentrations of the nano-complex was determined using the online calculator provided by AAT Bioquest.

RNA extraction and cDNA synthesis

The SINA kit (RNAXPLUS Cat No: RN7713C) and its methodology were used to extract the RNA from the treated and control cells, and the SINAclon cDNA synthesis kit (Cat No: RT5201) and reverse transcriptase enzyme were prepared in accordance with the manufacturer's instructions. Briefly, two microliters of 5X PCR buffer, one microlitre each of dNTP and oligo-dT, 0.5 microliters of reverse transcriptase enzyme, and 100 nanograms of the tested RNA were needed for cDNA synthesis.

Real Time PCR

The StepOnePlusTM Real-Time PCR System from Corbett Company was used to carry out the Real-Time PCR experiment. In this work, the expression of the apoptosis-related genes P53, BCl2, BAK, Bim, caspase 9 and caspase 8 was examined. GAPDH2 was utilized as an internal reference gene. For primer design, the sequences of the examined genes were first chosen from the website http://www.ncbi.nlm.nih.gov, and then particular forward and reverse primers for each gene were generated using oligo primer design software. Table No. 1 displays each gene's sequence. After designing forward and reverse primers with Primer 3 software, BLAST was performed using the NCBI website. The reaction was carried out in triplicate in a volume of 10 µl. It contained 2 microliters of RNase-free water, 1 microliter of cDNA, 5 microliters of Master MixesSYBR Green, and 0.5 microliters of each primer.

Hoechst staining for apoptosis analysis

In this work, cell death and apoptosis were examined using a fluorescence microscope with Hoechst 33285 staining. For this, MCF7 cells were exposed for 24 hours to a quadruple magnetic nano-complex at a determined LC50 concentration. After the incubation period, the culture media was removed, and the cell layer was washed with FBS buffer. The layer of the cell was fixed using paraformaldehyde. The cell layer was then coated with a diluted solution of Hoechst dye 33258 after being washed one more with FBS buffer. It was put on a microscope slide as a drop. The cells covered on the slide were examined using a fluorescent microscope after the smear preparation.

Conclusion

This study demonstrates the inhibitory and apoptotic properties of natural compounds and their synergistic effect in treating cancer cells, particularly in the form of their nanoformula. This is made

possible by the ability of the nanostructure to penetrate the cells on the one hand and the transfer of large amounts due to the greater surface area of the nanoparticle on the other.

Declarations

Acknowledgments

The authors are grateful to Islamic Azad University, Ahar Branch for their affectionate collaboration.

Author's Contribution: M.Z designed and outlined the framework of this experiment. Sh.Sh administered the test which was performed in Sahar laborarory (Ardebil,Iran), Ghazi Hospital (Tabriz, Iran), and Razi Institute (Tehran, Iran). All authors have observed and approved the final manuscript.

Data Availability

All data generated or analyzed during this study are included in this published article.

Conflict of Interests:

The authors proclaim that they have no conflicts of interest.

Funding/Support: The study was financially supported by the Islamic Azad University, Ahar Branch.

References

1. Yap KM, Sekar M, Fuloria S, Wu YS, Gan SH, Mat Rani NNI, et al. Drug Delivery of Natural Products Through Nanocarriers for Effective Breast Cancer Therapy: A Comprehensive Review of Literature. Int J Nanomedicine. 2021;16:7891–941.
2. Tabarestani S, Noori-Daloii, M. MOLECULAR GENETICS, DIAGNOSIS AND TREATMENT OF BREAST CANCER: REVIEW ARTICLE. Journal of Sabzevar University of Medical Sciences. 2010;17(2).
3. Wawruszak A, Halasa M, Okon E, Kukula-Koch W, Stepulak A. Valproic Acid and Breast Cancer: State of the Art in 2021. Cancers (Basel). 2021;13(14).
4. Mohammad RM, Muqbil I, Lowe L, Yedjou C, Hsu HY, Lin LT, et al. Broad targeting of resistance to apoptosis in cancer. Semin Cancer Biol. 2015;35 Suppl(0):S78-S103.
5. Parton M, Dowsett M, Smith I. Studies of apoptosis in breast cancer. BMJ. 2001;322(7301):1528–32.
6. Yuan L, Cai Y, Zhang L, Liu S, Li P, Li X. Promoting Apoptosis, a Promising Way to Treat Breast Cancer With Natural Products: A Comprehensive Review. Front Pharmacol. 2021;12:801662.
7. Krajewski S, Krajewska M, Turner BC, Pratt C, Howard B, Zapata JM, et al. Prognostic significance of apoptosis regulators in breast cancer. Endocr Relat Cancer. 1999;6(1):29–40.
8. Abe R, Beckett J, Abe R, Nixon A, Rochier A, Yamashita N, et al. Olive oil polyphenol oleuropein inhibits smooth muscle cell proliferation. Eur J Vasc Endovasc Surg. 2011;41(6):814–20.

9. Hassan ZK, Elamin MH, Daghestani MH, Omer SA, Al-Olayan EM, Elobeid MA, et al. Oleuropein induces anti-metastatic effects in breast cancer. Asian Pac J Cancer Prev. 2012;13(9):4555–9.
10. Chairez-Ramirez MH, de la Cruz-Lopez KG, Garcia-Carranca A. Polyphenols as Antitumor Agents Targeting Key Players in Cancer-Driving Signaling Pathways. Front Pharmacol. 2021;12:710304.
11. Wahle KW, Brown I, Rotondo D, Heys SD. Plant phenolics in the prevention and treatment of cancer. Adv Exp Med Biol. 2010;698:36–51.
12. Briguglio G CC, Pollicino M, Giambo F, Catania S,Fenga C. Polyphenols in cancer prevention:New insights. International Journal of Functional Nutrition. 2020;1(2).
13. Silva C, Correia-Branco A, Andrade N, Ferreira AC, Soares ML, Sonveaux P, et al. Selective pro-apoptotic and antimigratory effects of polyphenol complex catechin:lysine 1:2 in breast, pancreatic and colorectal cancer cell lines. Eur J Pharmacol. 2019;859:172533.
14. Anand S, Sowbhagya R, Ansari MA, Alzohairy MA, Alomary MN, Almalik AI, et al. Polyphenols and Their Nanoformulations: Protective Effects against Human Diseases. Life (Basel). 2022;12(10).
15. Davatgaran-Taghipour Y, Masoomzadeh S, Farzaei MH, Bahramsoltani R, Karimi-Soureh Z, Rahimi R, et al. Polyphenol nanoformulations for cancer therapy: experimental evidence and clinical perspective. Int J Nanomedicine. 2017;12:2689–702.
16. Hami Z SA. Synthesis and loading of nanocurcumin on iron magnetic nanoparticles modified with chitosan. Tehran Univ Med J. 2020;77(11):715–9.
17. Barzegar F, Zaefizadeh, M., Yari, R., & Salehzadeh, A. Synthesis of Nano-paramagnetic oleuropein to induce KRAS over-expression: Anew mechanism to inhibit AGS cancer cells. Medicina. 2019;55(7):388.
18. Zhou W, Feng X, Han H, Guo S, Wang G. Synergistic effects of combined treatment with histone deacetylase inhibitor suberoylanilide hydroxamic acid and TRAIL on human breast cancer cells. Sci Rep. 2016;6:28004.
19. Kupeli Akkol E, Genc Y, Karpuz B, Sobarzo-Sanchez E, Capasso R. Coumarins and Coumarin-Related Compounds in Pharmacotherapy of Cancer. Cancers (Basel). 2020;12(7).
20. Yang J, Liu X, Bhalla K, Kim CN, Ibrado AM, Cai J, et al. Prevention of apoptosis by Bcl-2: release of cytochrome c from mitochondria blocked. Science. 1997;275(5303):1129–32.
21. Bhattacharyya SS, Paul S, De A, Das D, Samadder A, Boujedaini N, et al. Poly (lactide-co-glycolide) acid nanoencapsulation of a synthetic coumarin: cytotoxicity and bio-distribution in mice, in cancer cell line and interaction with calf thymus DNA as target. Toxicol Appl Pharmacol. 2011;253(3):270–81.
22. Lee YK, Hwang JT, Kwon DY, Surh YJ, Park OJ. Induction of apoptosis by quercetin is mediated through AMPKalpha1/ASK1/p38 pathway. Cancer Lett. 2010;292(2):228–36.
23. Rauf A, Imran M, Khan IA, Ur-Rehman M, Gilani SA, Mehmood Z, et al. Anticancer potential of quercetin: A comprehensive review. Phytother Res. 2018;32(11):2109–30.

24. Shahbazi R DH, Esmaeili S. The anticancer effects of flavonoids: involvment of PI3K/ Akt signaling pathway. Iranian J Nutr Sci Food Technol. 2013;7(4).
25. Zang X, Cheng M, Zhang X, Chen X. Quercetin nanoformulations: a promising strategy for tumor therapy. Food Funct. 2021;12(15):6664–81.
26. Iannelli F, Roca MS, Lombardi R, Ciardiello C, Grumetti L, De Rienzo S, et al. Synergistic antitumor interaction of valproic acid and simvastatin sensitizes prostate cancer to docetaxel by targeting CSCs compartment via YAP inhibition. J Exp Clin Cancer Res. 2020;39(1):213.
27. Sanaei M, Kavoosi F. Effect of Valproic Acid on the Class I Histone Deacetylase 1, 2 and 3, Tumor Suppressor Genes p21WAF1/CIP1 and p53, and Intrinsic Mitochondrial Apoptotic Pathway, Pro- (Bax, Bak, and Bim) and anti- (Bcl-2, Bcl-xL, and Mcl-1) Apoptotic Genes Expression, Cell Viability, and Apoptosis Induction in Hepatocellular Carcinoma HepG2 Cell Line. Asian Pac J Cancer Prev. 2021;22(S1):89–95.
28. Ozman Z, Ozbek Iptec B, Sahin E, Guney Eskiler G, Deveci Ozkan A, Kaleli S. Regulation of valproic acid induced EMT by AKT/GSK3beta/beta-catenin signaling pathway in triple negative breast cancer. Mol Biol Rep. 2021;48(2):1335–43.
29. Gonet T, Maher BA, Kukutschova J. Source apportionment of magnetite particles in roadside airborne particulate matter. Sci Total Environ. 2021;752:141828.
30. Dutta RKS, P.K.; Pandey, A.C.. Design and surface modification of potential luminomagnetic nanocarriers for biomedical applications. J Nanopart Res. 2010;12(4):1211–9.
31. Mancarella S, Greco V, Baldassarre F, Vergara D, Maffia M, Leporatti S. Polymer-Coated Magnetic Nanoparticles for Curcumin Delivery to Cancer Cells. Macromol Biosci. 2015;15(10):1365–74.
32. Zhang R WC, Wang X, Sun Q, Chen B, Li X, Gutmann S, Lv G. Enhancement effect of nano Fe3O4 to the drug accumulation of doxorubicin in cancer cells. Materials Science and Engineering. 2009;29(5):1697–701.
33. Wang MS, Chen L, Xiong YQ, Xu J, Wang JP, Meng ZL. Iron oxide magnetic nanoparticles combined with actein suppress non-small-cell lung cancer growth in a p53-dependent manner. Int J Nanomedicine. 2017;12:7627–51.
34. Di Pompo G, Salerno M, Rotili D, Valente S, Zwergel C, Avnet S, et al. Novel histone deacetylase inhibitors induce growth arrest, apoptosis, and differentiation in sarcoma cancer stem cells. J Med Chem. 2015;58(9):4073–9.
35. Ahmad Farooqi A, Fayyaz S, Silva AS, Sureda A, Nabavi SF, Mocan A, et al. Oleuropein and Cancer Chemoprevention: The Link is Hot. Molecules. 2017;22(5).
36. Liu L, Ahn KS, Shanmugam MK, Wang H, Shen H, Arfuso F, et al. Oleuropein induces apoptosis via abrogating NF-kappaB activation cascade in estrogen receptor-negative breast cancer cells. J Cell Biochem. 2019;120(3):4504–13.
37. Manca MLL, F.; Pireddu, R.; Valenti, D.; Schlich, M.; Pini, E.; Ailuno, G.; Fadda, A.M.; Sinico, C.. Impact of nanosizing on dermal delivery and antioxidant activity of quercetin nanocrystals. J Drug Deliv Sci Technol. 2020;55:101482.

38. Utama K, Khamto N, Meepowpan P, Aobchey P, Kantapan J, Sringarm K, et al. Effects of 2',4'-Dihydroxy-6'-methoxy-3',5'-dimethylchalcone from Syzygium nervosum Seeds on Antiproliferative, DNA Damage, Cell Cycle Arrest, and Apoptosis in Human Cervical Cancer Cell Lines. Molecules. 2022;27(4).
39. Yadav N, Tripathi AK, Parveen A. PLGA-Quercetin Nano-Formulation Inhibits Cancer Progression via Mitochondrial Dependent Caspase-3,7 and Independent FoxO1 Activation with Concomitant PI3K/AKT Suppression. Pharmaceutics. 2022;14(7).
40. Salakou S, Kardamakis D, Tsamandas AC, Zolota V, Apostolakis E, Tzelepi V, et al. Increased Bax/Bcl-2 ratio up-regulates caspase-3 and increases apoptosis in the thymus of patients with myasthenia gravis. In Vivo. 2007;21(1):123–32.
41. Amaral C, Varela C, Borges M, Tavares da Silva E, Roleira FMF, Correia-da-Silva G, et al. Steroidal aromatase inhibitors inhibit growth of hormone-dependent breast cancer cells by inducing cell cycle arrest and apoptosis. Apoptosis. 2013;18(11):1426–36.
42. Rahal BA, Bardaweel SK. Implications and Efficacy of Aromatase Inhibitors in Combination and Monotherapy for the Treatment of Lung Cancer. Anticancer Agents Med Chem. 2022;22(18):3114–24.

Figures

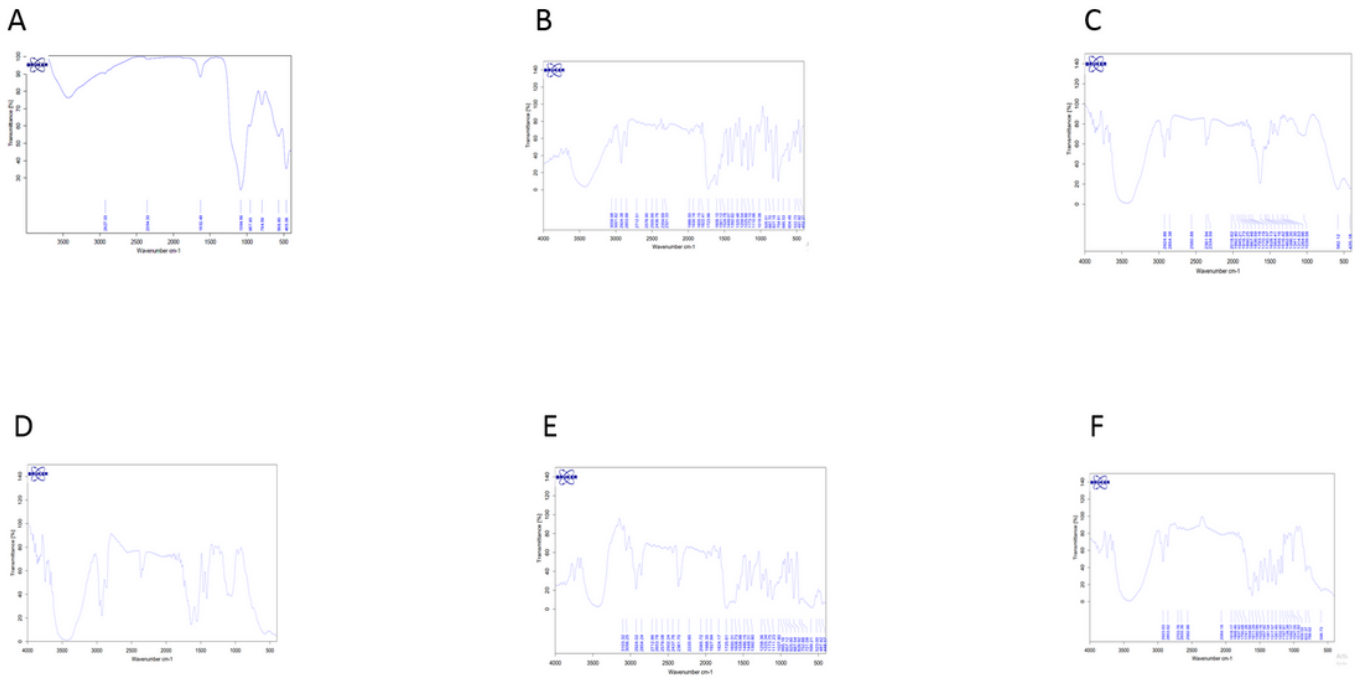

Figure 1

FT-IR spectrum of nano oleuropein (C), coumarin nanoparticles (D), valproic acid nanoparticles (F), Quercetin(G) nanoparticles attached to magnetite particles modified with 3-aminopropyltrimethoxysilane.

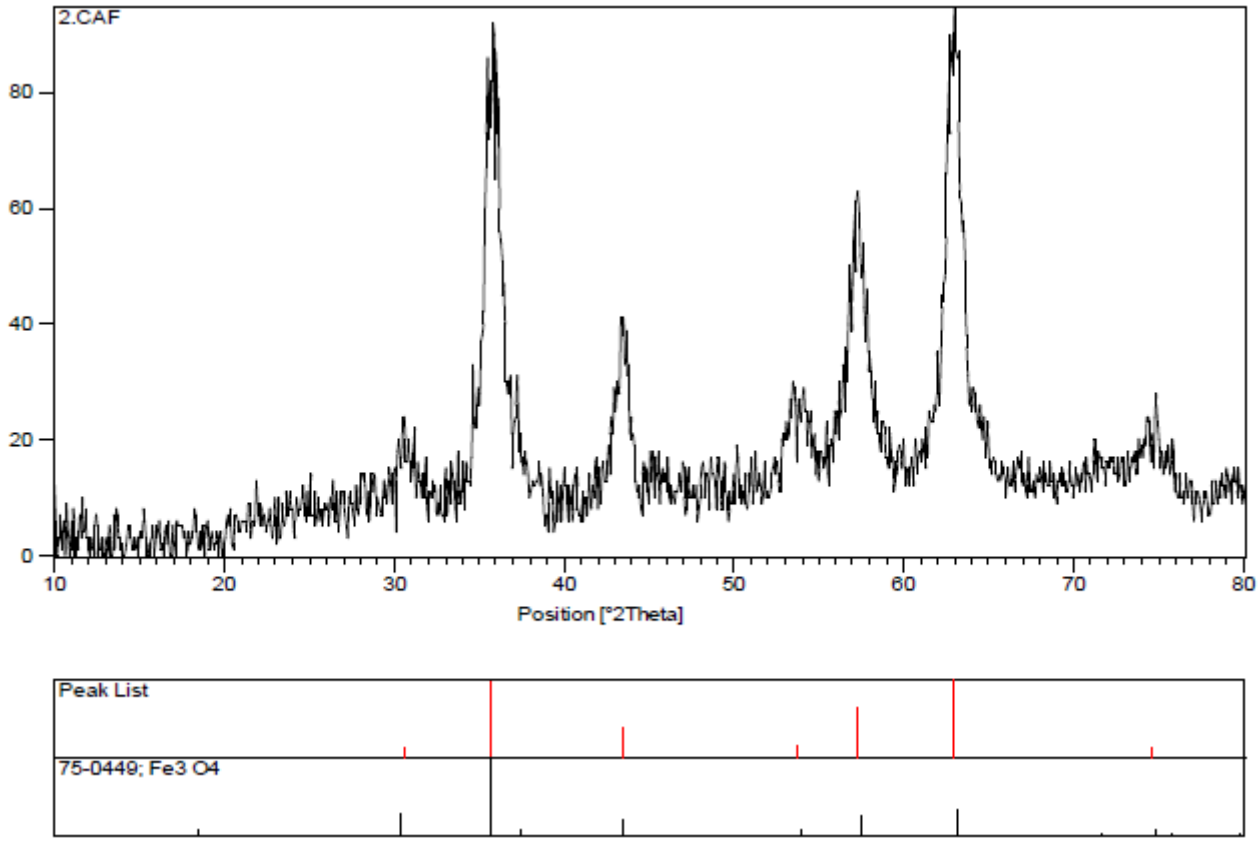

Figure 2

An XRD pattern associated with modified magnetite nanoparticles connected to compound 4 by 3-aminopropyltrimethoxysilane.

15	1550	68.78059	49.78059
16	1700	70.28317	51.28317
17	1850	71.49913	52.49913
18	2000	72.51551	53.51551
19	3000	75.80351	56.80351
20	4000	77.34667	58.34667
21	5000	78.08547	59.08547
22	6000	78.50502	59.50502
23	7000	78.79038	59.79038
24	8000	78.9722	59.9722
25	9000	79.10127	60.10127
26	10000	79.20066	60.20066
27	11000	79.26763	60.26763
28	12000	79.33128	60.33128
29	11000	79.32995	60.32995
30	10000	79.35064	60.35064
31	9000	79.31986	60.31986
32	8000	79.22367	60.22367
33	7000	79.04502	60.04502
34	6000	78.786	59.786
35	5000	78.38032	59.38032
36	4000	77.67354	58.67354
37	3000	76.23955	57.23955
38	2000	72.75838	53.75838
39	1850	71.92958	52.92958
40	1700	70.75163	51.75163
41	1550	69.28261	50.28261
42	1400	67.45601	48.45601
43	1250	65.13942	46.13942
44	1100	62.15411	43.15411

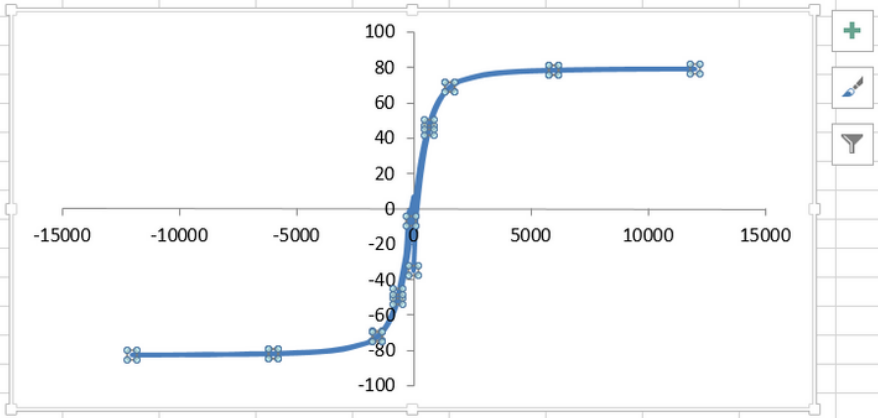

Figure 3

The magnetization curve for the field of 3-aminopropyltrimethoxysilane-modified magnetite iron oxide nanoparticles connected to the quadruple complex.

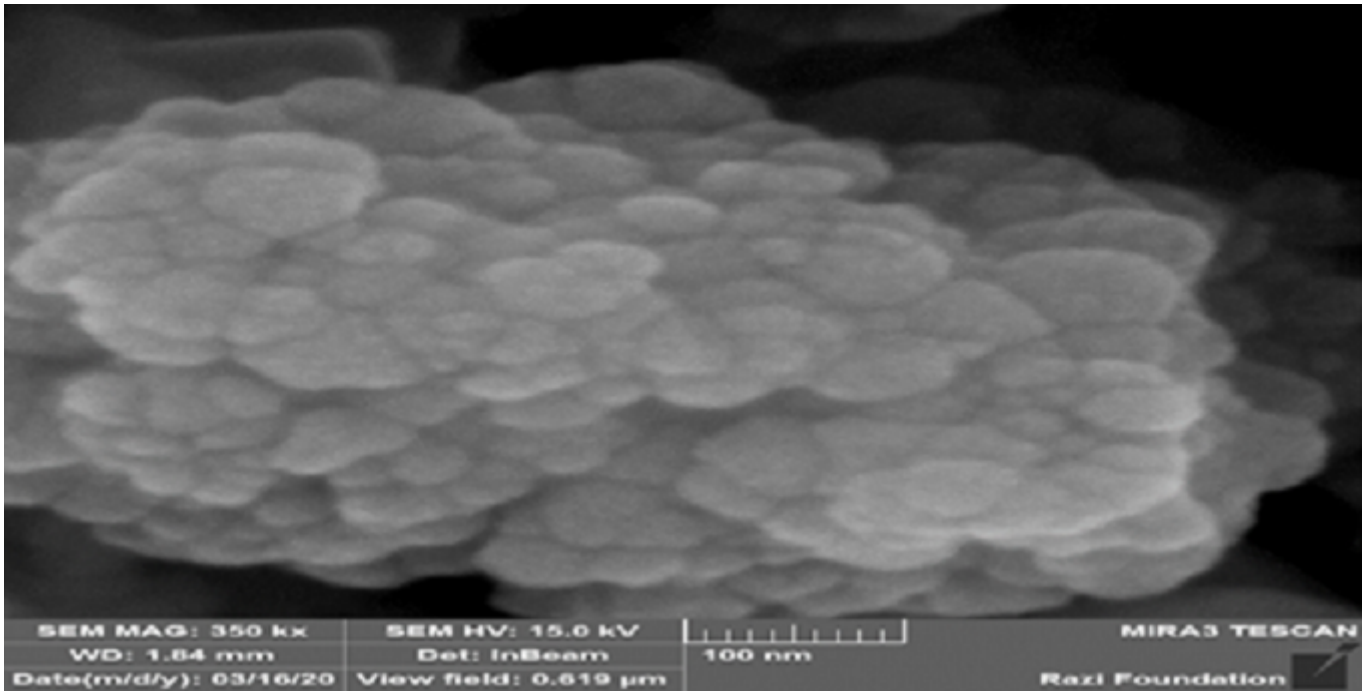

Figure 4

SEM images at a magnification of 100 nm of magnetite nanoparticles modified with 3-aminopropyltrimethoxysilane and attached to four compounds.

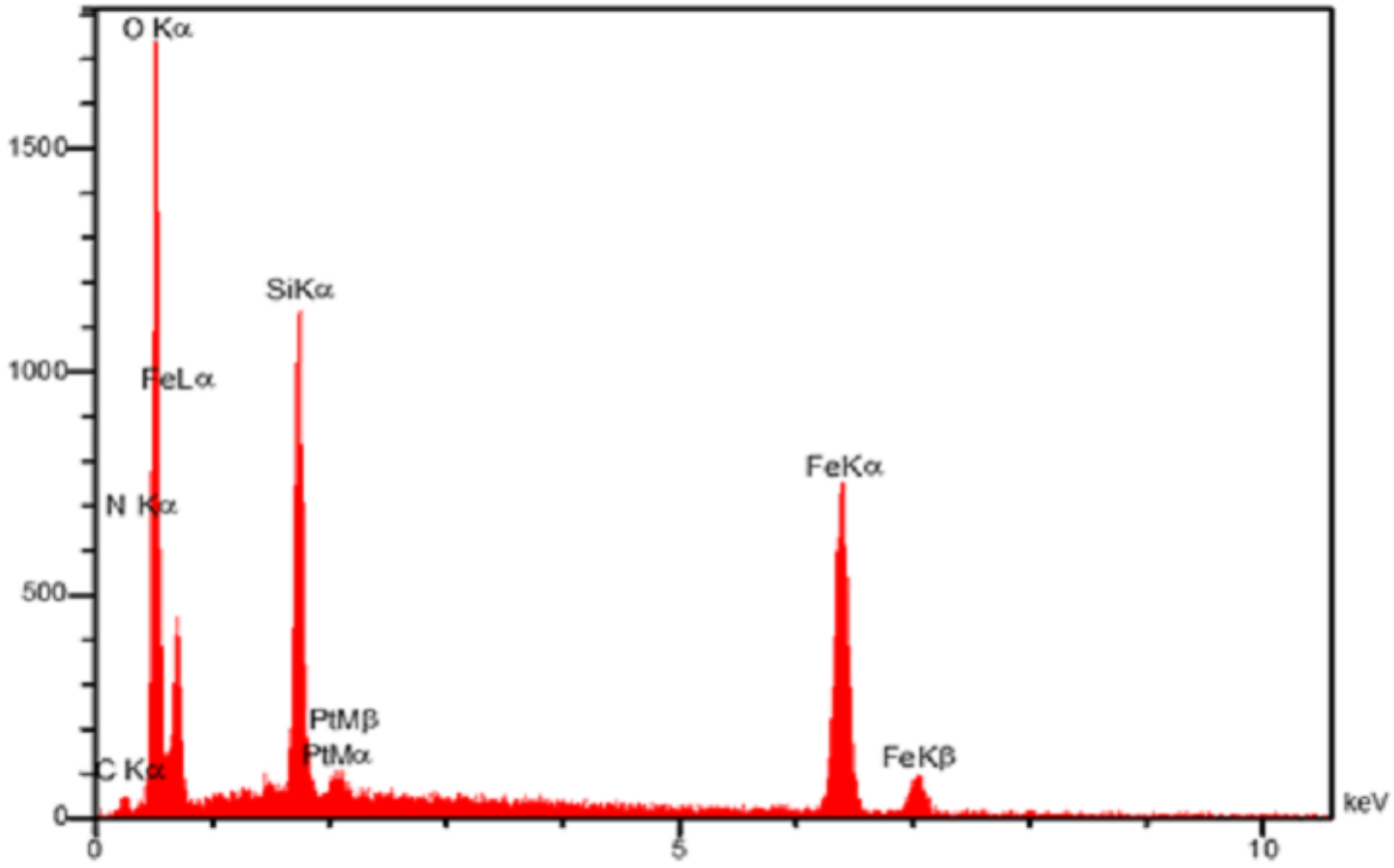

Figure 5

EDAX images of four compounds attached to magnetite iron oxide nanoparticles modified with 3-aminopropyltrimethoxysilane.

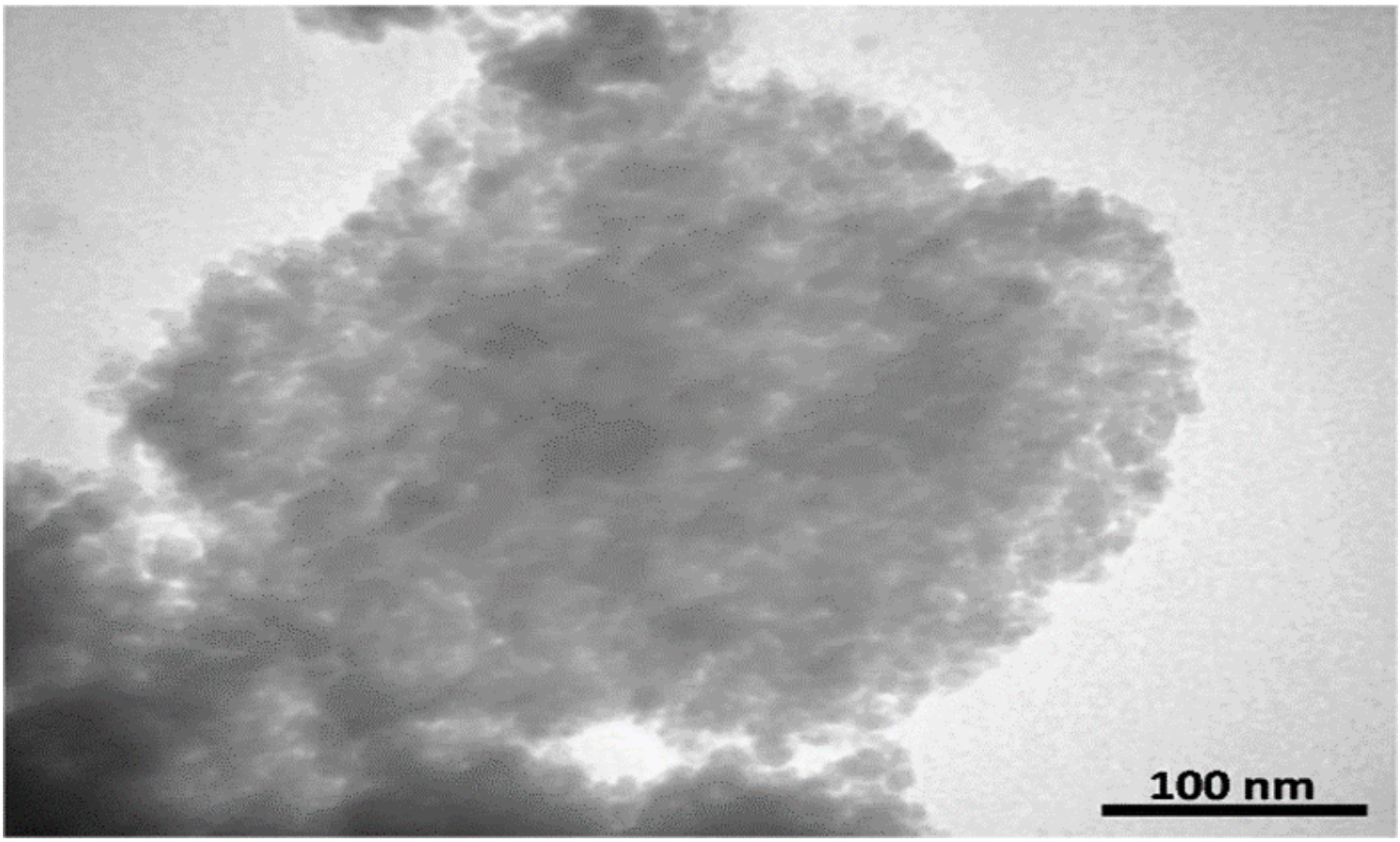

Figure 6

TEM image of magnetic nanocomposite.

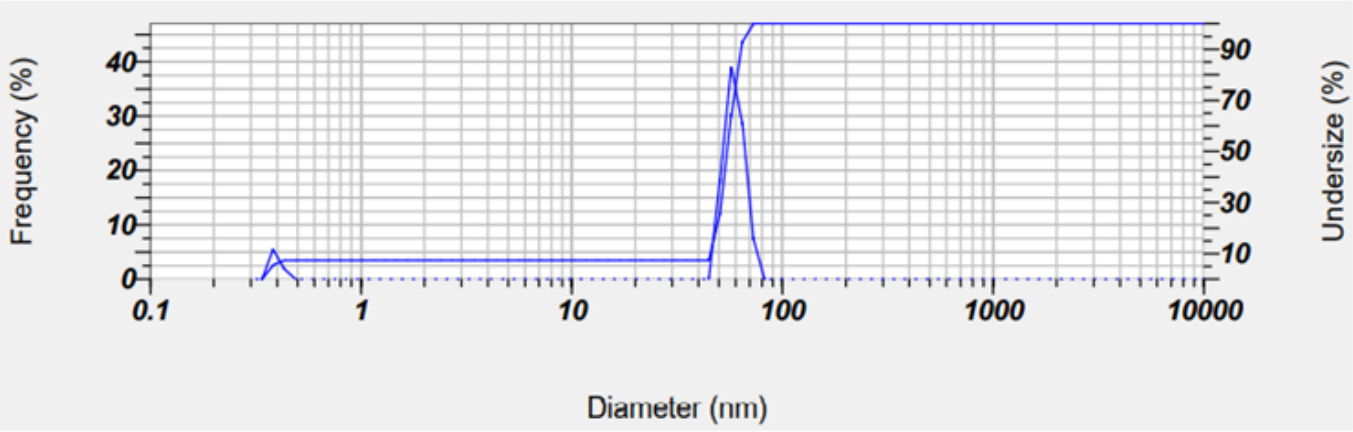

Figure 7

Nanoparticle size synthesized by DLS.

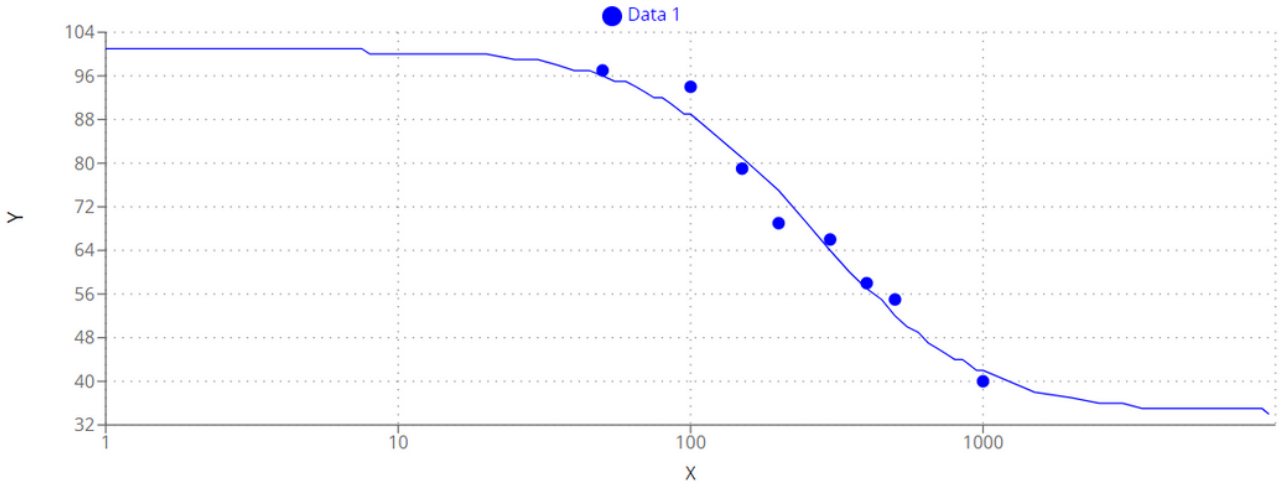

LC_{50} Regression Results [Data 1]

Parameter	Value
LC_{50}	264.6226
Equation	$Y = 34.2289 + \frac{100.7776 - 34.2289}{1 + \left(\frac{X}{264.6226}\right)^{1.5477}}$
Equation Form	$Y = Min + \frac{Max - Min}{1 + \left(\frac{X}{LC_{50}}\right)^{Hill\ coefficient}}$

LC_{50} Regression Calculator [Data 1]

Figure 8

LC50 curve for the quadruple magnetic nanocomposite.

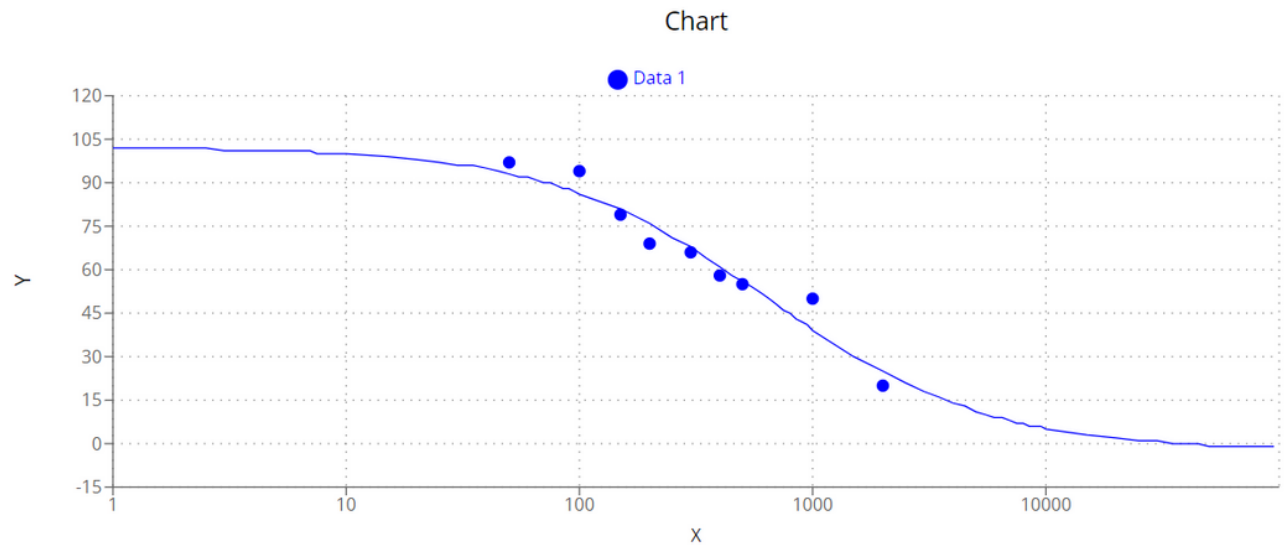

LC_{50} Regression Results [Data 1]

Parameter	Value
LC_{50}	644.654
Equation	$Y = -2.3638 + \frac{102.1613 + -2.3638}{1 + (\frac{X}{644.654})^{0.9234}}$
Equation Form	$Y = Min + \frac{Max - Min}{1 + (\frac{X}{LC_{50}})^{Hill\ coefficient}}$

Figure 9

LC50 curve for the quadruple physical composition.

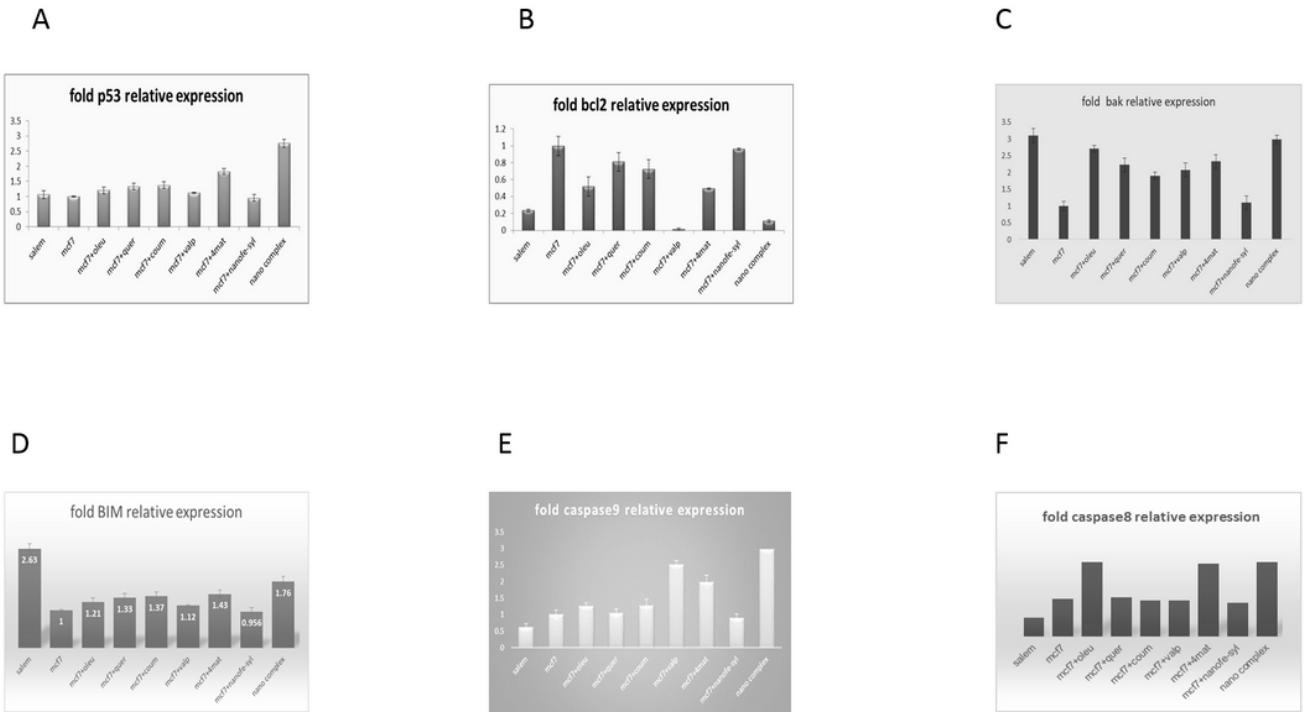

Figure 10

The relative expression level of bcl2, p53, BIM, bak, caspase8 and caspase 9 in treated cells.

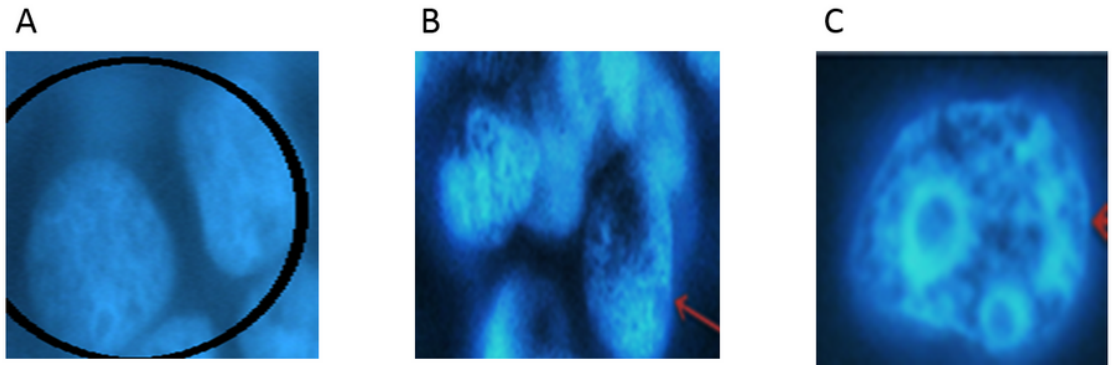

Figure 11

The results of Hoechst staining of apoptotic cells - A - untreated MCF7 cells B - apoptotic MCF7 cells treated with quadruple magnetite nano-complex and C - treated with oleuropein

Supplementary Files

This is a list of supplementary files associated with this preprint. Click to download.

- supplementary.docx